DETRA NOTE

DETRA NOTE 2021-1

A HEALTH-JARROW-MORTON MODEL COMPLIANT WITH SOLVENCY II? PROMISES AND PITFALLS

By Simon Boigelot & Donatien Hainaut

Detralytics

DISCLAIMER

The content of the Detra Notes for a pedagogical use only. Each business case is so specific that a careful analysis of the situation is needed before implementing a possible solution. Therefore, Detralytics does not accept any liability for any commercial use of the present document. Of course, the entire team remain available if the techniques presented in this Detra Note required your attention.

Detralytics
Rue Belliard/Belliardstraat 2
1040 Brussels
www.detralytics.com
info@detralytics.eu

ABSTRACT

In this working paper, we adapt the Heath-Jarrow Morton (HJM) framework by considering a constraint of convergence of future forward rates toward a constant exogeneous rate set e.g. by a regulator. This limit rate, called “ultimate forward risk” or UFR, was introduced by the EIOPA in 2015 to extrapolate the initial yield curve for maturities beyond the last liquid point. We show that adding a constraint of convergence in the HJM model impacts not only the term structure of interest rates but also the future variance of zero-coupon bonds.

Contents

1 Introduction

The Solvency II directive recommends to evaluate the Best Estimate Liabilities (BEL) as the sum of expected discounted future cash-flows. To discount liabilities cash-flows, an appropriate term structure of discount factors is needed. From the no arbitrage pricing theory, the zero rates related to the stochastic discount factors have to be risk-free, e.g. free from any counterparty risks.

There is no easy answer to the question of defining such a risk-free rate. Today in Solvency II, the discount rates are based on interest rates swaps (IRS) adjusted by a credit spread. The construction of this swap curve relies on the Smith-Wilson (SW) method (2001), described in the EIOPA (2015) technical specifications. Beyond a chosen maturity - the last liquid point (LLP), currently 20 years -, the forward rate is forced by regulatory rules, to converge with an exogenously specified speed to a fixed long term level called the Ultimate Forward Rate (UFR).

This assumption of convergence is questionable as underlined by Jorgensen (2018). Nevertheless, if we admit it, the interest rate model used for simulations of future cash-flows should also generate forward rates converging on average toward the UFR. There exist multiple approaches for interest rate modeling and we refer the reader to the book of Brigo and Mercurio (2016) or to Rebonato (2004) for a survey of methods. This article focuses on the Heath Jarrow Morton framework (1990) which is is a standard in the industry since at least two decades. It encompasses a wide variety of approaches like the Hull-White or the G2++ models. This article adapts the HJM framework in order to force the convergence of future forward rates toward the UFR. We show that adding such a constraint has various consequences on the term structure of zero-coupon bond variances. Firstly, the shape of this term structure is fully determined by the function driving the convergence of forward rates to the UFR in order to avoid arbitrages. Secondly, the curve of zero-coupon bond variances converges at long term to zero. This slightly decreases the value at risks of very long term bonds or liabilities. Thirdly, the adapted HJM model cannot anymore explain flips from positive to negative values observed for some principal components of the yield covariance matrix. Last but not least, the empirical illustration does not allow to conclude to a fast convergence of forward rates to an ultimate one contrary to what is stated in the current version of Solvency II.

The paper is structured as follows. We start by reviewing the main properties of the Heath Jarrow Morton model. The next section summarizes the procedure to estimate parameters under the real measure with a principal component analysis. This approach is illustrated in Section 4 with a dataset of swap rates from 2014 to 2020. In Section 5, we adapt the HJM framework to ensure the convergence of forward rates to a constant UFR at long term. Section 6 and 7 respectively provide a numerical illustration and a multivariate extension.

2 Heath-Jarrow-Morton (HJM) in a nutshell

We present in the next sections a very general framework in which the short term rate converges at long term to a constant ultimate forward rate (UFR). This is inspired from the Heath-Jarrow-Morton model (HJM 1990) that we review in this section. In such a setting, we consider an infinity of instantaneous forward processes, denoted by $f(t,T)$ where $0 \leq t \leq T$. Let us recall that $f(t,T)$ is is the interest rate in force at time t for a future investment or borrowing of duration dt at date T. The zero-coupon bond price of maturity T at time t is denoted by $P(t,T)$. Using standard non-arbitrage arguments, we can show that instantaneous forward rates are equal to

$$f(t,T) = -\frac{\partial \ln P(t,T)}{\partial T},$$

or alternatively that $P(t,T) = \exp\left(-\int_t^T f(t,s)ds\right)$. On the other hand, the instantaneous risk-free rate is a stochastic process denoted by $(r_t)_{t\geq 0}$ defined on a probability space $\left(\Omega, (\mathcal{F}_t)_{t\geq 0}, \mathbb{Q}\right)$ that is such that

$$P(t,T) \;=\; \mathbb{E}^{\mathbb{Q}}\left(e^{-\int_t^T r_s ds} \,|\, \mathcal{F}_t\right).$$

By construction, the risk free rate is such that $r_t = f(t,t)$. We denote by $\boldsymbol{W}_t = (W_t^1, ..., W_t^p)^\top$ a vector of p-Brownian motions defined on Ω, endowed with the natural filtration of $\boldsymbol{W}_t$ noted $\{\mathcal{F}_t\}_{t\geq 0}$ and a risk neutral probability measure $\mathbb{Q}$. For a fixed maturity T, $f(t,T)$ is an Itô process driven by the next SDE:

$$df(u,T) = \alpha(u,T)du + \boldsymbol{\sigma}(u,T)^\top d\boldsymbol{W}_u, \tag{2.1}$$

where the drift $\alpha(u,T)$ and the p-vector $\boldsymbol{\sigma}(u,T) = (\sigma_1(u,T), ..., \sigma_p(u,T))^\top$ are $\mathcal{F}_u$-adapted processes. To ensure that forward rate processes are well defined, we require that $\int_0^T |\alpha(u,T)|du$ and $\int_0^T |\sigma_i^2(u,T)|du$ for $i = 1, ..., p$ are finite almost surely. Therefore, the forward rate admits the integral representation:

$$f(t,T) \;=\; f(0,T) + \int_0^t \alpha(u,T)du + \int_0^t \boldsymbol{\sigma}(u,T)^\top d\boldsymbol{W}_u, \tag{2.2}$$

whereas the risk-free rate is:

$$r_t \;=\; f(0,t) + \int_0^t \alpha(u,t)du + \int_0^t \boldsymbol{\sigma}(u,t)^\top d\boldsymbol{W}_u. \tag{2.3}$$

Under the assumption that $\int_0^T \int_0^s |\alpha(u,s)|\, du\, ds$ is finite, the zero-coupon bond price is equal to

$$\begin{aligned} P(t,T) &= \exp\left(-\int_t^T f(t,s)ds\right) \\ &= \exp\left(-\int_t^T f(0,s)ds - \int_0^t \int_t^T \alpha(u,s)ds\, du - \int_0^t \int_t^T \boldsymbol{\sigma}(u,s)^\top ds\, d\boldsymbol{W}_u\right). \end{aligned} \tag{2.4}$$

The cash account is denoted by $(B_t)_{t\geq 0}$. This is the value of a deposit of one monetary unit capitalized at risk-free rate till time t: $B_t = \exp\left(\int_0^t r_s ds\right)$. Since $r_s = f(s,s)$, this cash account is also equal to

$$B_t \;=\; \exp\left(\int_0^t f(0,s)ds + \int_0^t \int_u^t \alpha(u,s)ds\,du + \int_0^t \int_u^t \boldsymbol{\sigma}(u,s)^\top ds\, d\boldsymbol{W}_u\right). \tag{2.5}$$

The next proposition introduces a condition on the drift of forward rates that guarantees the absence of arbitrage.

Proposition 1. *If the market is arbitrage free then the drift of forward rates $\alpha(t,T)$ is related to $\sigma(t,T)$ by the next relation:*

$$\alpha(t,T) \;=\; \boldsymbol{\sigma}(t,T)^\top \int_t^T \boldsymbol{\sigma}(t,u)\,du\,. \tag{2.6}$$

Proof. Under the risk neutral measure $\mathbb{Q}$, discounted prices are martingales. In our framework the discount factor is B_t^{-1} and from Equations (2.4) and (2.6), the discounted bond price is equal to:

$$\frac{P(t,T)}{B_t} \;=\; \exp\left(-\int_0^T f(0,s)ds - \int_0^t \int_u^T \alpha(u,s)dsdu + \int_0^t \boldsymbol{S}(u,T)^\top d\boldsymbol{W}_u\right)$$

where $\boldsymbol{S}(u,T)$ is a p-vector, integral of $\boldsymbol{\sigma}(u,s)$:

$$\boldsymbol{S}(u,T) \;=\; -\int_u^T \boldsymbol{\sigma}(u,s)\,ds\,.$$

The discounted bond price is a martingale if and only if the drift of $d\left(\frac{P(t,T)}{B_t}\right)$ is null. By the Itô's lemma, this differential is

$$\frac{d\left(\frac{P(t,T)}{B_t}\right)}{\frac{P(t,T)}{B_t}} \;=\; \left(\frac{1}{2}\boldsymbol{S}(t,T)^\top \boldsymbol{S}(t,T) - \int_t^T \alpha(t,s)ds\right)dt + \boldsymbol{S}(t,T)^\top d\boldsymbol{W}_t\,. \tag{2.7}$$

The drift is null if and only if $\int_t^T \alpha(t,s)ds = \frac{1}{2}\boldsymbol{S}(t,T)^\top \boldsymbol{S}(t,T)$. Deriving this last equality with respect to T leads to the condition (2.6). □

A direct consequence of this last proposition is that the zero-coupon bonds earns on average the risk-free rate under $\mathbb{Q}$.

Corollary 2. *Under the risk neutral measure, the zero-coupon bond is solution of the SDE:*

$$\frac{dP(t,T)}{P(t,T)} = r_t dt - \left(\int_t^T \boldsymbol{\sigma}(t,s)ds\right)^\top d\boldsymbol{W}_t\,. \tag{2.8}$$

for $t \leq T$.

Proof. By construction, the bond price is such that $P(t,T) = \exp\left(-\int_t^T f(t,s)ds\right)$ and

$$\begin{aligned} d\left(-\int_t^T f(t,s)ds\right) &= f(t,t)dt - \int_t^T df(t,s)ds \\ &= \left(r_t - \int_t^T \alpha(t,s)ds\right)dt - \left(\int_t^T \boldsymbol{\sigma}(t,s)^\top ds\right) d\boldsymbol{W}_t\,. \end{aligned}$$

Then using the Itô's lemma with the variable $-\int_t^T f(t,s)ds$ leads to

$$\begin{aligned} \frac{dP(t,T)}{P(t,T)} &= \left(r_t \underbrace{- \int_t^T \alpha(t,s)ds + \frac{1}{2}\left(\int_t^T \boldsymbol{\sigma}(t,s)ds\right)^\top \left(\int_t^T \boldsymbol{\sigma}(t,s)ds\right)}_{=0}\right) dt \\ &\quad - \left(\int_t^T \sigma(t,s)ds\right)^\top d\boldsymbol{W}_t\,, \end{aligned}$$

where we have used the condition (2.6). □

3 Econometric estimation of the HJM model

Models used for risk management have to generate sample paths for interest rates that are compliant with the observed behaviour of financial markets. This explains why parameters are estimated from time-series sampled under the real measure, denoted by $\mathbb{P}$. On the contrary, models used for option pricing must foremost replicate the current market prices on a given day. In this case, we need instead to estimate parameters under the risk neutral measure $\mathbb{Q}$. This is usually performed by minimizing the mean square error between market and modeled prices of a sample of derivatives. This section focuses on the first case and proposes an estimation procedure under the real measure $\mathbb{P}$.

Under the assumption that forward rates are ruled by Equation (2.1), we infer that forward rates are solutions of the following SDE under the real measure

$$df(u,T) = \left(\alpha(u,T) + \boldsymbol{\sigma}(u,T)^\top \boldsymbol{\theta}_u\right) du + \boldsymbol{\sigma}(u,T)^\top d\tilde{\boldsymbol{W}}_u\,, \tag{3.1}$$

where $\boldsymbol{\theta}_u = (\theta_u^1, \ldots, \theta_u^p)^\top$ is a p-vector of $\mathcal{F}_t$-adapted processes and $\tilde{\boldsymbol{W}}_u = \boldsymbol{W}_u - \boldsymbol{\theta}_u$ is a p-vector of Brownian motions under $\mathbb{P}$. Informally, the vector $\boldsymbol{\theta}_u$ defines the market risk premiums of each risk factors. The change of measure from $\mathbb{P}$ to $\mathbb{Q}$ is defined by the following Radon-Nykodym derivatives

$$\left.\frac{d\mathbb{Q}}{d\mathbb{P}}\right|_t = \exp\left(-\int_0^t \boldsymbol{\theta}_s^\top d\tilde{\boldsymbol{W}}_s - \frac{1}{2}\int_0^t ||\boldsymbol{\theta}_s||^2 ds\right).$$

We denote by $\gamma(u,T) = \alpha(u,T) + \boldsymbol{\sigma}(u,T)^\top \boldsymbol{\theta}_u$ the drift of forward rates under the real measure and rewrite the forward rate of maturity $t+\tau$ under $\mathbb{P}$

$$f(t,t+\tau) \;=\; f(0,t+\tau) + \int_0^t \gamma(u,t+\tau)\,du + \int_0^t \boldsymbol{\sigma}(u,t+\tau)^\top d\tilde{\boldsymbol{W}}_u\,.$$

In order to estimate the model, we need the dynamics of zero-coupon bond prices under $\mathbb{P}$. At time t, the bond price of maturity $t+\tau$ is related to forward rates by the relation $P(t,t+\tau) = \exp\left(-\int_t^{t+\tau} f(t,s)ds\right)$. The differential of the integral of forward rates is:

$$\begin{aligned} d\ln P(t,t+\tau) &= f(t,t)dt - \int_t^{t+\tau} df(t,s)ds \\ &= \left(r_t - \int_t^{t+\tau} \gamma(t,s)ds\right)dt - \left(\int_t^{t+\tau} \boldsymbol{\sigma}(t,s)^\top ds\right) d\tilde{\boldsymbol{W}}_t\,. \end{aligned} \tag{3.2}$$

If we remember the definition of $\gamma(t,s)$ and condition (2.6), using the Itô's lemma with the state variable $\ln P(t,t+\tau)$ allows us to prove that $P(t,t+\tau)$ is a geometric Brownian motion

$$\begin{aligned} \frac{dP(t,t+\tau)}{P(t,t+\tau)} \;=\; & \left(r_t - \int_t^{t+\tau} \boldsymbol{\sigma}(t,s)^\top \boldsymbol{\theta}_t ds\right)dt \\ & - \left(\int_t^{t+\tau} \boldsymbol{\sigma}(t,s)ds\right)^\top d\tilde{\boldsymbol{W}}_t\;. \end{aligned}$$

In order to estimate parameters under $\mathbb{P}$, we assume that the drift of $\ln P(t,t+\tau)$ is stationary and then does not depends upon t:

$$r_t - \int_t^{t+\tau} \gamma(t,s)ds \approx g(\tau)\,.$$

This assumption is strong but is commonly accepted by practioners. Let us assume that we sample $d \geq p$ bonds prices at $n+1$ equispaced times $\{t_0,...,t_n\}$. The interval between two successive sampling times is Δ whereas the maturities of bond prices are denoted $\{\tau_1,...,\tau_d\}$. Firstly, we calculate the first order differences of log-bond prices (the yield):

$$y_i(\tau_j) = \ln P\left(t_{i+1}, t_{i+1}+\tau_j\right) - \ln P\left(t_i, t_i+\tau_j\right) \qquad i = 1\ldots n\,,\; j = 1,\ldots,d\,.$$

According to Equation (3.2), the vector $\boldsymbol{y}_i = \left(y_i(\tau_j)\right)_{j=1,...,d}$ is the realization of a multivariate random variable $\boldsymbol{Y} = \{Y_1,...,Y_d\}$ of yields where

$$Y_j = g(\tau_j)\Delta - \left(\int_t^{t+\tau_j} \boldsymbol{\sigma}(t,s)^\top ds\right)\left(\tilde{\boldsymbol{W}}_{t+\Delta} - \tilde{\boldsymbol{W}}_t\right)\; j = 1,...,d. \tag{3.3}$$

This last equation emphasizes that functions $\boldsymbol{\sigma}(.,.)$ define the covariance matrix of $\boldsymbol{Y}$. For this reason, we calculate the $d \times d$ empirical covariance matrix of $(\boldsymbol{y}_i)_{i=1,...,n}$ and denote it by Σ. The matrix Σ is positive definite and symmetric. Then it admits the following representation

$$\Sigma \;=\; \Psi\, \Lambda\, \Psi^\top ,$$

where Ψ is the $d \times d$ matrix of normed right eigenvectors, $\Psi = (\Psi_1, \ldots, \Psi_d)$ of the covariance matrix. The $\Psi_k = (\Psi_{k,1}, ..., \Psi_{k,d})^\top$ are vectors of dimension d. $\Lambda = \text{diag}\,(\lambda_1, ..., \lambda_d)$ is the diagonal matrix of ordered eigenvalues such that:

$$\lambda_1 \geq \lambda_2 \geq \ldots \geq \lambda_d \,.$$

The occurrence of $\boldsymbol{Y}$ form a cloud of points in a d dimensions space. The eigenvectors define an new orthonormal basis and the variance of the cloud of points is maximal in each axis direction. The coordinates of observations $\boldsymbol{y}_i$ in this new basis are given by:

$$\begin{pmatrix} \Psi_1^\top \boldsymbol{y}_i \\ \vdots \\ \Psi_d^\top \boldsymbol{y}_i \end{pmatrix} \quad i = 1, ..., n \,.$$

The origin of the orthonormal basis is an estimate of the expectation of $\boldsymbol{Y}$, $\bar{\boldsymbol{y}} = (\bar{y}_1, ..., \bar{y}_d)^\top = \frac{1}{n}\sum_{i=1}^n \boldsymbol{y}_i$. Whereas an estimate of variance along each axis is the associated eigenvalues:

$$\mathbb{E}\left(\widehat{\left(\Psi_j^\top \boldsymbol{Y} - \Psi_j^\top \mathbb{E}\,(\boldsymbol{Y})\right)^2}\right) = \lambda_j \quad j = 1, ..., d \,.$$

The total variance is the sum of variances along axis: $\sum_{j=1}^d \lambda_j$. In practice, a projection of the cloud of $(\boldsymbol{y}_i)_{i=1,...,n}$ in a subspace spanned by the two or three largest eigenvalues, is sufficient to explain more than 90% of the total variance. James and Weber (2000, Chapter 16) found that two factors explain about 95% of the variation in the term structure movements. Buhler et al. (1999) carry out an empirical study of one and two-factor Heath, Jarrow, and Morton type models along with one and two-factor inversion type models. Let us imagine that we perform this projection on a subspace of dimension p. In this case, the distribution of $\boldsymbol{Y}$ can be approximated by

$$Y_j \;\approx\; \bar{y}_j + \sum_{k=1}^{p} \Psi_{j,k}\, \sqrt{\lambda_k}\, X_k \quad , \; j = 1, ..., d \tag{3.4}$$

where X_k are p independent normal random variables, $N\left(0, \sqrt{\Delta}\right)$. A comparison of Equations (3.3) and (3.4) reveals that an estimator $\widehat{\boldsymbol{\sigma}}(t,s) = \left(\widehat{\sigma}_k(t,s)\right)_{k=1,...,p}$ of $\boldsymbol{\sigma}(t,s)$ must minimize the spreads between $\Psi_{j,k}\sqrt{\lambda_k}$ and $-\int_t^{t+\tau_j} \sigma_k(t,s)ds$ for all $j \in \{1, ..., d\}$:

$$\widehat{\sigma}_k(.,.) \;=\; \arg\min_{\sigma_k(.,.)} \sum_{j=1}^{d} \left(-\int_t^{t+\tau_j} \sigma_k(t,s)ds - \Psi_{j,k}\sqrt{\lambda_k} \right)^2 \quad k = 1, ..., p \,. \tag{3.5}$$

In practice, we choose a-priori a functional form for $\sigma_k(t,s)$ and estimate parameters of this function by least square minimization of the above criterion. This method is illustrated in the next section.

4 Numerical Illustration

In order to illustrate this section, we fit the HJM model to zero-coupon yields bootstrapped from ICE swap rates in Euro from the Federal Reserve bank of St Louis[1]. The period ranges from the 1/8/2014 to the 21/2/2020. Tenors run from 1 year to 30 years ($d = 30$). The yields for missing tenors are interpolated with natural cubic splines. We consider a model with two Brownian motions, $p = 2$, and that forward rates are solution of:

$$df(t,T) = \alpha(t,T)dt + \sigma_1(t,T)dW_t^1 + \sigma_2(t,T)dW_t^2 \tag{4.1}$$

where $\sigma_1(.)$ is constant and $\sigma_2(.)$ is the product of a linear function and a decreasing exponential

$$\begin{aligned} \sigma_1(t,t+\tau) &= \sigma_1\,, \\ \sigma_2(t,t+\tau) &= \sigma_2(1+\beta_1\tau)e^{-\beta_2\tau}\,. \end{aligned} \tag{4.2}$$

Notice that Amin and Morton (1994) analysed six specifications for the volatility function of the forward rates in a Heath, Jarrow, and Morton framework. In order to estimate the four parameters $(\sigma_1, \sigma_2, \beta_1, \beta_2)$, we integrate these volatility functions over $[t, t+\tau]$:

$$\begin{aligned} &\int_t^{t+\tau} \sigma_1(t,s)ds = \sigma_1\,\tau\,, \\ &\int_t^{t+\tau} \sigma_2(t,s)ds = \sigma_2\left(\frac{\beta_1+\beta_2}{\beta_2^2}\left(1-e^{-\beta_2\tau}\right) - \frac{\beta_1}{\beta_2}\tau\, e^{-\beta_2\tau}\right)\,. \end{aligned} \tag{4.3}$$

The estimate $\widehat{\sigma}_1$ of σ_1 is obtained by minimization of Equation (3.5):

$$\widehat{\sigma}_1 = \arg\min_{\sigma_1} \sum_{j=1}^{30} \left(-\sigma_1\,\tau_j - \Psi_{j,1}\sqrt{\lambda_1}\right)^2\,,$$

where Ψ_1 is the normed eigenvector associated to the largest eigenvalue, λ_1 of the matrix of covariance Σ. This first component explains 99.12% of the total variance of $\boldsymbol{Y}$. The estimate $\widehat{\sigma}_2$, $\widehat{\beta}_1$, $\widehat{\beta}_2$ of σ_2, β_1 and β_2 are obtained in a similar manner:

$$\begin{aligned} \widehat{\sigma}_2, \widehat{\beta}_1, \widehat{\beta}_2 = \arg\min_{\sigma_2,\beta_1,\beta_2} \sum_{j=1}^{30} \Bigg(-\sigma_2 \Bigg(&\frac{\beta_1+\beta_2}{\beta_2^2}\left(1-e^{-\beta_2\tau}\right) - \\ &\frac{\beta_1}{\beta_2}\tau\, e^{-\beta_2\tau}\Bigg) - \Psi_{j,2}\sqrt{\lambda_2}\Bigg)^2\,, \end{aligned}$$

where Ψ_2 is the normed eigenvector associated to the second largest eigenvalue of Σ. This component explain 0.77% of the total variance. Estimates are reported in Table 4.1. $\widehat{\sigma}_1$ and $\widehat{\sigma}_2$ are

[1] https://fred.stlouisfed.org/

respectively around 3 and 1 basis points whereas $\widehat{\beta}_1$, $\widehat{\beta}_2$ are negative. Figure 4.1 compares the integrated volatilities (4.3) to their empirical counterparts. These graphs confirms the excellent fit provided by functions (4.2).

Parameters	Estimates
$\widehat{\sigma}_1$	0.0003617341
$\widehat{\sigma}_2$	0.0001714276
$\widehat{\beta}_1$	-0.0999049663
$\widehat{\beta}_2$	0.0308140508

Table 4.1: Estimates of parameters for volatility functions 4.2.

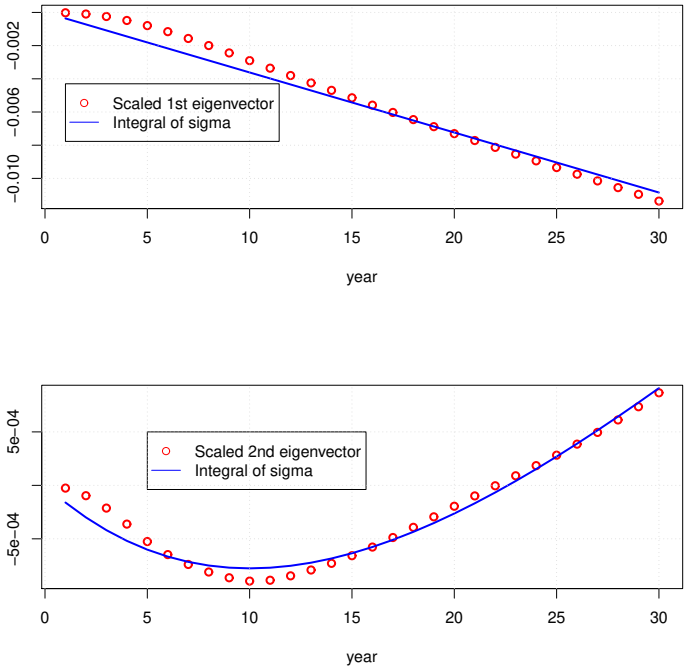

Figure 4.1: Comparison of $\Psi_{j,k}\sqrt{\lambda_k}$ and $-\int_t^{t+\tau_j}\sigma_k(t,s)ds$ for $k=1,2$ and $\tau_j=1,...,30$ years.

5 A one-factor HJM model converging to the UFR

In Solvency II, long term interest rates and then forward rates converge to an ultimate forward rate (UFR) that we denote by f_∞ in the sequel. This ultimate forward rate is computed as an

average of past 1 year real rates summed up to the targeted inflation in the Eurozone. The EIOPA calculates the UFR as follows:

$$f_\infty = \frac{1}{n}\sum_{k=1960}^{A} y_k + \text{inflation target}\,,$$

where A is the last elapsed calendar year and y_k is the annual real rate for year k (the real rate is the nominal rate minus the inflation). This real rate is the equally weighted average of real rates for seven countries chosen by EIOPA. In 2020, the UFR was $f_\infty = 3.75\%$. if we admit this assumption, the interest rate model used for simulations of future cash-flows should also generate forward rates converging on average toward the UFR. We show in this section how to adapt the HJM model in order to force the convergence of forward rates to f_∞. In particular, we require that the expectation of future forward rates converge to the UFR as follows

$$\lim_{t\to\infty} \mathbb{E}^{\mathbb{Q}}\left(f(t,t+\tau)\right) = f_\infty \quad \forall\, \tau \geq 0. \tag{5.1}$$

This constraint is not fulfilled in the HJM framework. To see this, let us consider a HJM model and assume that volatility functions $\boldsymbol{\sigma}(u,s)$ are deterministic functions of times u and s. Under the EIOPA assumption that $\lim_{t\to\infty} f(0,t) = f_\infty$, we infer from Equation (2.2) and Proposition 1 that forward rates converge to:

$$\lim_{t\to\infty} \mathbb{E}^{\mathbb{Q}}\left(f(t,t+\tau)\right) \;=\; f_\infty + \lim_{t\to\infty} \mathbb{E}^{\mathbb{Q}}\left(\int_0^t \boldsymbol{\sigma}(u,t+\tau)^\top \int_u^{t+\tau} \boldsymbol{\sigma}(u,s)\, dsdu\right).$$

The second term of the right hand side of this equation is not null and therefore forward rates do not tend to f_∞. Another argument in favour of modifying the HJM framework is that $\mathbb{E}^{\mathbb{Q}}\left(f(t,t+\tau)\right)$ does not converge to a finite value in many circumstances. To see this, let us consider a one factor HJM model. We have seen in the previous section that a good fit of the first principal component is achieved with a constant volatility function, i.e. $\boldsymbol{\sigma}(u,s) = \sigma_1$. In this case, the expected instantaneous forward rate is equal to

$$\begin{aligned}\mathbb{E}^{\mathbb{Q}}\left(f(t,t+\tau)\right) &= f(0,t+\tau) + \mathbb{E}^{\mathbb{Q}}\left(\int_0^t \sigma_1 \int_u^{t+\tau} \sigma_1\, dsdu\right)\\ &= f(0,t+\tau) + \sigma_1^2\left(\frac{1}{2}t^2 + \tau t\right),\end{aligned}$$

and tends to infinity when $t \to \infty$. The quadratic growth of forward rates with time also implies that long term liabilities are on average less expensive in the future than today (at least if σ_1^2 is significantly different from zero). This has a direct impact on the calculation of the capital solvency requirement (CSR) at a future date $t >> 0$.

In order to ensure the convergence of forward rates, we consider a continuous differentiable function, $h(t,T) : \mathbb{R}^{2,+} \to [0,1]$ such that $h(0,T) = 0$ and $\lim_{t\to\infty} h(t,T) = 1$ for all $T \geq t$. We call

$h(t,T)$ as the "convergence function". The HJM model in adapted in the following manner. We assume that instantaneous forward rates are equal to

$$f(t,T) = f(0,T) + h(t,T)\left(f_\infty - f(0,T)\right) + \int_0^t \sigma(u,T)dW_u\,, \tag{5.2}$$

where $(W_t)_{t\geq 0}$ is a Brownian motion and $\sigma(u,T)$ is a $\mathcal{F}_u$-adapted process. By construction, the condition (5.1) of convergence to the UFR is well fulfilled. We assume that $h(t,T)$ is separable with respect to t and T in the sense that we can rewrite them as a product of two functions $h(t,T) = h_1(t)h_2(T)$ with the following conditions:

$$h_1(0) = 0\,,\ \lim_{t\to\infty} h_1(t) = 1\,,\ \lim_{T\to\infty} h_2(T) = 1\,.$$

In the empirical illustrations, we consider three convergence functions. The first one is independent from T and is an exponential concave function of t:

$$h(t,T) = h_1(t) = \left(1 - e^{-\beta_0 t}\right)\,. \tag{5.3}$$

In the second case, the convergence function $h(t,T)$ is the product of

$$\begin{cases} h_1(t) &= \left(1 - e^{-\beta_0 t}\right)\,, \\ h_2(T) &= \left(1 - e^{-\beta_1 (T-\beta_2)^2}\right)\,. \end{cases} \tag{5.4}$$

The last function that we consider, is very similar to the second one excepted that it depends on the fourth power of T:

$$\begin{cases} h_1(t) &= \left(1 - e^{-\beta_0 t}\right)\,, \\ h_2(T) &= \left(1 - e^{-\beta_1 (T-\beta_2)^4}\right)\,. \end{cases} \tag{5.5}$$

The model such as defined by Equation (5.2) is not arbitrage free. We will see that arbitrages may be avoided if and only if the variance of forward rates takes a specific form. If we refer to Equation (2.1), we can reframe our model into the HJM framework if $\int_0^t \alpha(u,T)du$ is equal to the product of $h(t,T)$ and the spread between f_∞ and $f(0,T)$:

$$\int_0^t \alpha(u,T)du = h(t,T)\left(f_\infty - f(0,T)\right)\,.$$

Since the function $h(t,T)$ is differentiable with respect to t, the function $\alpha(.,.)$ is equal to

$$\alpha(t,T) = \frac{\partial h(t,T)}{\partial t}\left(f_\infty - f(0,T)\right)\,. \tag{5.6}$$

We use this relation in order to find the expression of the volatility function that ensures the absence of arbitrage.

Proposition 3. *The model (5.2) is arbitrage-free if and only the volatility function is equal to:*

$$\sigma(t,T) = \pm \frac{\frac{\partial h(t,T)}{\partial t}\left(f_\infty - f(0,T)\right)}{\sqrt{2\left(f_\infty \int_t^T \frac{\partial h(t,s)}{\partial t} ds - \int_t^T \frac{\partial h(t,s)}{\partial t} f(0,s) ds\right)}}\,. \tag{5.7}$$

If $h(t,T) = h_1(t)$ is independent from T, then

$$\sigma(t,T) = \pm \frac{\frac{\partial h_1(t)}{\partial t}\left(f_\infty - f(0,T)\right)}{\sqrt{2\frac{\partial h_1(t)}{\partial t}\left(f_\infty\left(T-t\right) + \ln\frac{P(0,T)}{P(0,t)}\right)}}\,, \tag{5.8}$$

for all $t \leq T$.

Proof. From Equation (5.6), we infer that the integral of $\alpha(t,s)$ from t to T is equal to

$$\int_t^T \alpha(t,s) ds \;=\; f_\infty \int_t^T \frac{\partial h(t,s)}{\partial t} ds - \int_t^T \frac{\partial h(t,s)}{\partial t} f(0,s) ds\,, \tag{5.9}$$

On the other hand, Proposition 1 states that $\int_t^T \alpha(t,s) ds = \frac{1}{2}\left(\int_t^T \sigma(t,s)\, ds\right)^2$ in absence of arbitrages. Therefore the integral of the volatility function becomes

$$\int_t^T \sigma(t,s) ds \;=\; \pm\sqrt{2\left(f_\infty \int_t^T \frac{\partial h(t,s)}{\partial t} ds - \int_t^T \frac{\partial h(t,s)}{\partial t} f(0,s) ds\right)}\,.$$

Deriving this last expression with respect to the expiry T leads to Equation (5.7). If $h(t,T) = h_1(t)$ is independent from the expiry T , the second term in the right hand side of Equation (5.9) is rewritten as

$$\int_t^T \frac{\partial h(t,s)}{\partial t} f(0,s) ds = \frac{\partial h(t)}{\partial t} \int_t^T f(0,s) ds,$$

where the integral of forward rates is by definition equal to the log-ratio of two zero coupon bond prices:

$$\begin{aligned} -\int_t^T f(0,s) ds &= -\int_0^T f(0,u) du + \int_0^t f(0,u) du \\ &= \ln \frac{P(0,T)}{P(0,t)}\,. \end{aligned}$$

We infer from this last expression that

$$\int_t^T \alpha(t,s) ds \;=\; \frac{\partial h(t)}{\partial t} f_\infty \left(T-t\right) + \frac{\partial h(t)}{\partial t} \ln \frac{P(0,T)}{P(0,t)}\,. \tag{5.10}$$

from which we retrieve Equation (5.8). □

According to Corollary 2, the instantaneous volatility of bond prices is proportional to the integral $\int_t^T \sigma(t,s)ds$. From Equation (5.7), this integral is fully determined by the convergence function $h(t,T)$ and by the initial term structure of forward rates. Furthermore Equation (5.8) reveals that the ultimate forward rate, f_∞ , has to fulfill the following constraint

$$f_\infty \quad \geq \quad \frac{\int_t^T \frac{\partial h(t,s)}{\partial t} f(0,s)ds}{\int_t^T \frac{\partial h(t,s)}{\partial t} ds},$$

for all $T \geq t$. Otherwise the volatility function is not defined. A last important point concerns the asymptotic behaviour of the volatility function. As $\lim_{t\to\infty} h(t,T) = 1$, the first order derivative with respect to t converges to zero, i.e. $\lim_{t\to\infty} \frac{\partial h(t,T)}{\partial t} = 0$. As $\sigma(t,T)$ is directly proportional to this derivative, we infer that $\lim_{t\to\infty} \sigma(t,T) = 0$.

6 Estimation of the one-factor HJM-UFR model

To calibrate a HJM model, we select a priori a volatility function and the drift of forward rates under $\mathbb{Q}$ is then fully determined by these functions. This approach is inverted for a HJM-UFR model. We start by defining a convergence function $h(t,T)$, that drives forward rates. This choice fully determines the shape of the volatility function. We denote by $\boldsymbol{\beta} = \{\beta_0, \beta_1 ...\}$ the vectors of parameters involved in the definition of $h(t,T)$. If we intend to use this model under the real measure $\mathbb{P}$, the vector $\boldsymbol{\beta}$ is estimated in a similar manner to Section 3. Let us consider a data set of d zero-coupon bond prices of maturities $\tau_{j=1,...d}$. We denote by λ_1 the largest eigenvalue of the covariance matrix of first-order differences of log-bond prices. As previously, Ψ_1 is the eigenvector paired to λ_1. An estimator $\widehat{\boldsymbol{\beta}}$ under $\mathbb{P}$ is the set of parameters minimizing the spread between observed and modeled volatilities of zero-coupon bonds:

$$\widehat{\boldsymbol{\beta}} \quad = \quad \arg\min_{\boldsymbol{\beta}} \sum_{j=1}^{d} \left(- \int_t^{t+\tau_j} \sigma(t,s)\, ds - \Psi_{j,1} \sqrt{\lambda_1} \right)^2 . \tag{6.1}$$

The integrals $\int_t^{t+\tau_j} \sigma(t,s)ds$ are calculated with Equation (5.7). The integrals $\int_t^T \frac{\partial h(t,s)}{\partial t} ds$ and $\int_t^T \frac{\partial h(t,s)}{\partial t} f(0,s)ds$ are numerically computed.

As illustration, we apply this method to ICE swap rates in Euro from the 1/8/2014 to the 21/2/2020. We perform a principal component analysis of the covariance matrix of first-order differences of log-bond prices. Next, we solve the optimization problem (6.1) with $d = 30$ for convergence functions (5.3), (5.4) and (5.5). The reference date t, for the calculation of forward rates is set to the 21/2/2020.

Finally, we fit a Smith-Wilson model[2] to ICE swap rates in Euro on the 21/2/2020 (See appendix). We impose $f_\infty = 3.75\%$. The Smith-Wilson model serves to extrapolate swap rates and

[2]The Smith-Wilson model (2001) interpolates market swap rates for short term maturities and extrapolate the yield curve for long term maturities, using the ultimate forward rate. We refer the reader to the EIOPA technical note from 2015.

forward rate curves for maturities beyond 30 years. We use it to analyse the volatility of bond prices for maturities longer than 30 years. Forward rates calculated with the Smith-Wilson model converge at long term toward f_∞, i.e. $\lim_{\tau\to\infty} f(0,\tau) = 3.75\%$.

Parameter	$h(t,T)$		
Estimates	Eq. (5.3)	Eq. (5.4)	Eq. (5.5)
$\widehat{\beta_0}$	3.3759e-05	1.3357e-04	8.9420e-05
$\widehat{\beta_1}$		3.05710e-03	6.2140e-05
$\widehat{\beta_2}$		0.0000	1.4952e-03

Table 6.1: Parameter estimates of convergence functions (5.3), (5.4) and (5.5).

The parameter estimates are reported in Table 6.1 for the three convergence functions, (5.3), (5.4) and (5.5). Figure 6.1 compares $-\int_0^{\tau_j} \sigma(0,s)ds$ for τ_j ranging from 1 to 60 years and the $\Psi_{j,1}\sqrt{\lambda_1}$ for the first 30 years. The fit with the two convergence functions depending on T is excellent while the first one fails to replicate the trend of the scaled eigenvector. For convergence function (5.4) and (5.5), we observe an inflection point for maturities above 30 years: at long term, the curve of bond volatilities tends to become flat. This figure also displays the zero-coupon bond volatilities at time $t = 30$ (i.e. $-\int_{30}^{30+\tau_j} \sigma(30,s)ds$) for maturities from 1 to 60 years. As mentioned at the end of the previous section, the whole term structure of volatilities slowly flattens to zero when t increases. This may be seen as an advantage or a drawback. Using the HJM-UFR model for long-term risk management ensures that bond volatilities will not explode with the time-horizon. On the contrary, we can also argue that we run the risk to underestimate the exposure to interest rates fluctuations at long term.

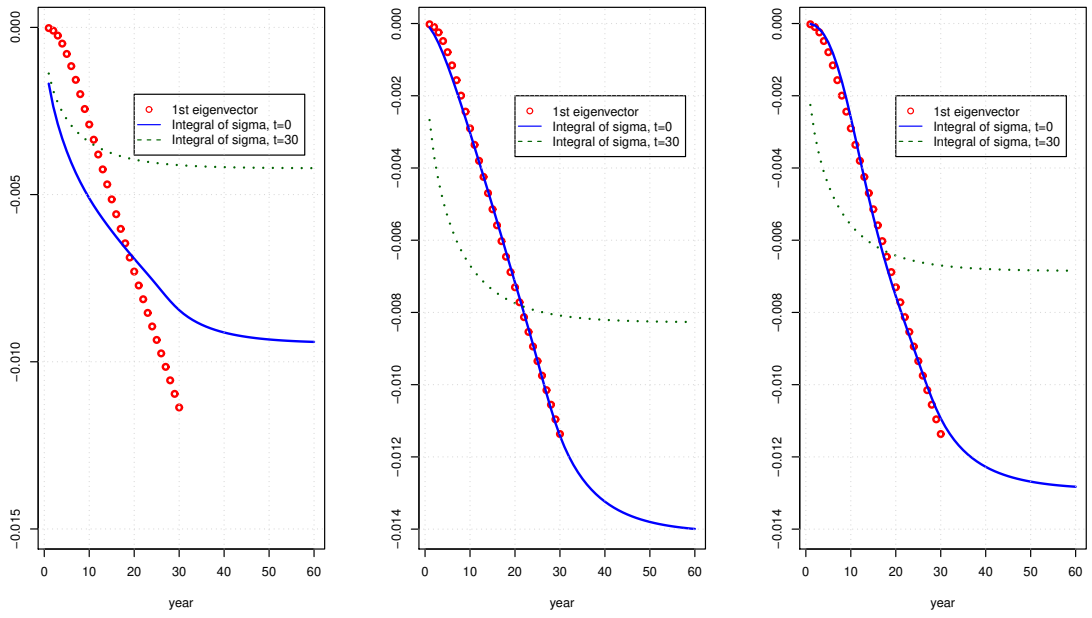

Figure 6.1: Comparison of $\Psi_{j,1}\sqrt{\lambda_1}$ and $-\int_0^{t+\tau_j}\sigma(0,s)ds$. Left, mid and right plots: $h(t,T)$ in Eq. (5.3), (5.4) and (5.5).

In Figure 6.2, we plot the estimated convergence function (5.4) at various dates and for various maturities. The right and left plots both reveal that the convergence of $h(t,T)$ to 1 when $t \to \infty$ and $T \to \infty$, is extremely slow. We can legitimately raise the question of the realism of the assumption made by EIOPA. In Solvency II, interest rates and forward rates converge to the UFR for maturities beyond 60 years. In our framework with the second convergence function, $h(t = 60, T = 80)$ =0.00175 which is very far from 1. Even after 1000 years, $h(t = 1000, T = 1020) = 0.0855$ is still very low! Our estimation procedure clearly emphasizes that it is impossible to reconciliate the assumption of quick convergence to an UFR with the observed term structure of bond volatilities. Combining a quick convergence and a realistic term structure of bond volatilities is possible only if we drop the assumption of absence of arbitrage. Jorgensen (2018) arrives to a similar conclusion but based on the analysis of the term structure of interest rates.

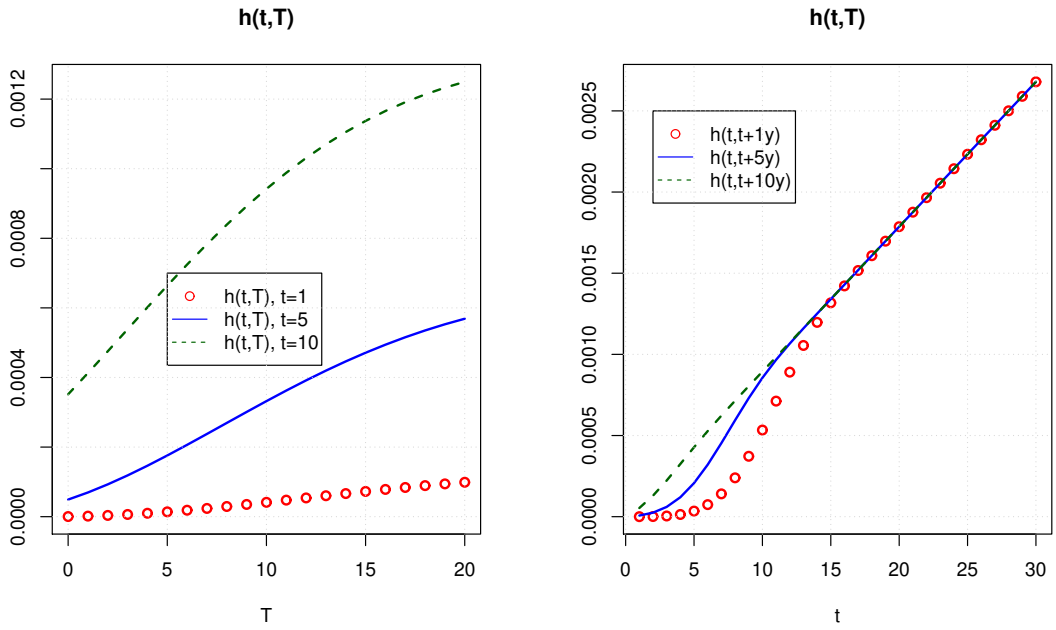

Figure 6.2: Convergence function $h(t,T)$, such as defined in Eq. (5.4) .

We compare next the expected forward rates to those computed with the 1-dimension HJM model. We denote by $\bar{f}_{UFR}(.,.)$, these expected rates obtained with the HJM UFR model:

$$\bar{f}_{UFR}(t,t+\tau) = \mathbb{E}^{\mathbb{Q}}\left(f(t,t+\tau)\right) = f(0,t+\tau) + h(t,t+\tau)\left(f_\infty - f(0,t+\tau)\right) ,$$

where $h(t,T)$ given by Equation (5.4). We denoted these rates by $\bar{f}_{HJM}(.,.)$ in the HJM model:

$$\bar{f}_{HJM}(t,t+\tau) = \mathbb{E}^{\mathbb{Q}}\left(f(t,t+\tau)\right) = f(0,t+\tau) + \sigma_1^2\left(\frac{1}{2}t^2 + \tau t\right) .$$

As mentioned earlier, $\lim_{t\to\infty}\mathbb{E}^{\mathbb{Q}}\left(f(t,t+\tau)\right) = +\infty$. Nevertheless, the estimate $\widehat{\sigma}_1 = 0.0003617341$ is very small and the convergence is then extremely slow. The right plot of Figure 6.3 shows the curves of $\bar{f}_{UFR}(t,t+\tau)$ for $t \in \{0,30,60,90\}$ and maturities from 1 to 20 years. We observe that expected forward rates converge after 60 years to a value slightly close to 3.75%. This is mainly due to the fact that forward rates calculated with the Smith-Wilson model converge toward f_∞, i.e. $\lim_{\tau\to\infty} f(0,\tau) = 3.75\%$. The term $h(t,t+\tau)\left(f_\infty - f(0,t+\tau)\right)$ slightly speed up the convergence. Since $\widehat{\sigma}_1$ is small, we do not observe a significant difference between $\bar{f}_{HJM}(t,t+\tau)$ and $\bar{f}_{UFR}(t,t+\tau)$ at least for t up to 100 years. The right plot of Figure 6.3 shows the spread between HJM and HJM-UFR expected forward rates. We see that this gap is equal to a few basis points.

Based on the previous analysis, we draw an interesting conclusion. In theory the HJM-UFR model guarantees the convergence of future forward rates to the UFR. It is in this sense more compliant with Solvency II than the HJM model. Nevertheless, due to current market conditions, we do not observe a wide gap between expected forward rates computed with both models. On

average, yield curves simulated with HJM or HJM-UFR will then be quasi similar! To our great surprise, the main visible difference concerns the term structure of bond volatilities. Within the 1D HJM framework, this volatility is linearly proportional to the maturity of the bond. Whereas in the 1D HJM-UFR model, the term structure of volatilities is curved and tends to be flat for maturities from 50 up to 80 years.

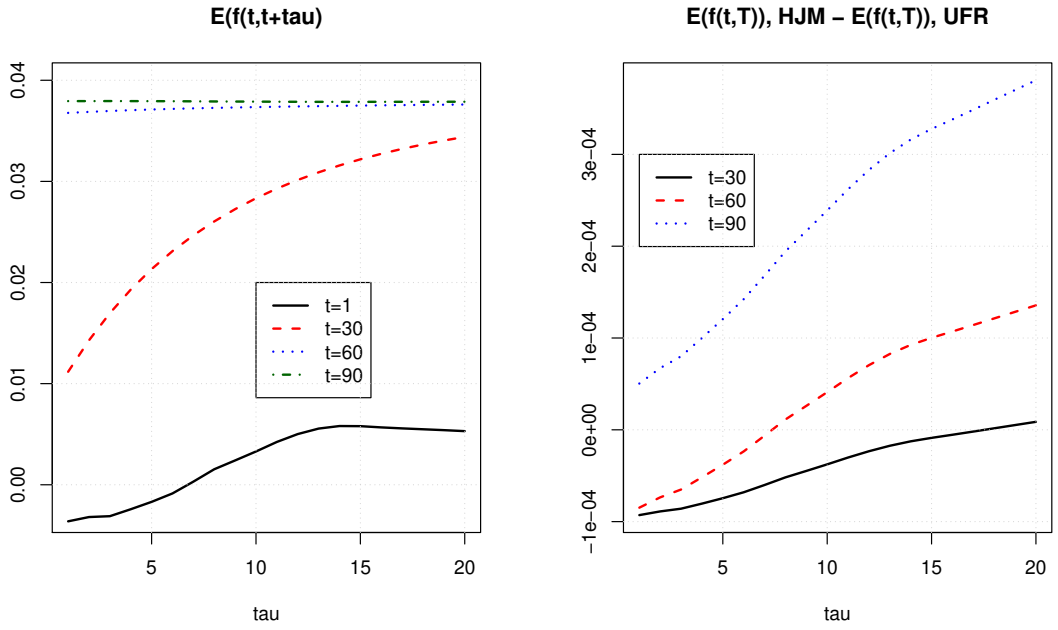

Figure 6.3: Convergence function $h(t,T)$, such as defined in Eq. (5.4) .

To conclude this section, we compare the distribution of simulated zero-coupon bond prices obtained with the one factor HJM and HJM-UFR models and parameter estimates of Tables 4.1, 6.1. We fit the Smith-Wilson curve to ICE swap rates in Euro on the 21/2/2020 from which we derive the term structure of forward rates. We impose $f_\infty = 3.75\%$ and work with the convergence function as in Equation (5.4). Given $h(t,T)$, $\alpha(t,T)$ and $\sigma(t,T)$ respectively take the forms described by Equations (5.6) and (5.7). We consider an equispaced time decomposition $\{t_0, ..., t_n\}$ such that the interval between two successive sampling times is $\Delta_t = 1/252$, a trading day. The following recurrence relation

$$f(t_{k+1},T) = f(t_k,T) + \alpha(t_k,T)\Delta_t + \sigma(t_k,T)(W_{t_k+\Delta_t} - W_{t_k}) \ , \tag{6.2}$$

for $k = 0$ to $n-1$ allows us to simulate one sample path of instantaneous forward rates both the HJM and HJM-UFR models. We run 10 000 Monte-Carlo simulations and denote the forward rates in the j^{th} scenario by $f^{(j)}(.,.)$ for $j = 1$ to 10 000. Let us recall that the zero coupon bond price of maturity T at time t is such that $P(t,T) = \exp\left(-\int_t^T f(t,s)ds\right)$. Discretizing this integral on the tenor axis with $m+1$ Δ_T-equispaced points, $T_0 = t < T_1 < ... < T_{k-1} < T_m = T$, leads to

the following approximation:

$$P^{(j)}(t,T) \approx \exp\left(-\sum_{i=0}^{m} f^{(j)}(t,T_i)\Delta_T\right) , \tag{6.3}$$

for $j = 1, ..., 10\,000$. We set $m = 100$ and consider bonds with maturities of 20, 30 and 40 years. Tables 6.2, 6.3 and 6.4 report the average and empirical percentiles of their prices after 1 and 30 days, 1, 5, 10 and 15 years. We also show the 99% relative values at risk (noted "99% Rel. VaR"). If $\bar{P}(t,T)$ and $P_{1\%}(t,T)$ are respectively the average and 1% percentile of simulated bond prices, this relative VaR is calculated as $\left(\bar{P}(t,T) - P_{1\%}(t,T)\right)/\bar{P}(t,T)$. For the 20 and 30 years bonds, the relative VaR are comparable at short term. At longer term (above 1 year), the UFR model leads to a higher VaR than the HJM. This difference raises up to 1.37% for the 30 years bond at $t = 15$y. In this sense, the HJM UFR is more conservative than the HJM model. The flattening of bond volatilities at long term only affects the 40 years bond for which the VaR computed with the HJM UFR model is smaller than the one obtained with the HJM framework, whatever the time horizon of the VaR.

$T = 20y$, HJM UFR	$t = 1d$	$t = 30d$	$t = 1y$	$t = 5y$	$t = 10y$	$t = 15y$
$\bar{P}(t,T)$	0.9604	0.9598	0.9561	0.9450	0.9486	0.9725
$P_{1\%}(t,T)$	0.9594	0.9544	0.9404	0.9150	0.9170	0.9500
$P_{5\%}(t,T)$	0.9597	0.9559	0.9451	0.9238	0.9266	0.9566
99% Rel. VaR	0.10%	0.57%	1.65%	3.17%	3.33%	2.32%
$T = 20y$, HJM	$t = 1d$	$t = 30d$	$t = 1y$	$t = 5y$	$t = 10y$	$t = 15y$
$\bar{P}(t,T)$	0.9604	0.9598	0.9561	0.9451	0.9485	0.9726
$P_{1\%}(t,T)$	0.9594	0.9542	0.9407	0.9188	0.9227	0.9571
$P_{5\%}(t,T)$	0.9597	0.9559	0.9454	0.9264	0.9308	0.9614
99% Rel. VaR	0.11%	0.59%	1.61%	2.79%	2.73%	1.59%

Table 6.2: Percentiles of a 20 years bond price with the HJM-UFR and HJM frameworks

$T = 30y$, HJM UFR	$t = 1d$	$t = 30d$	$t = 1y$	$t = 5y$	$t = 10y$	$t = 15y$
$\bar{P}(t,T)$	0.9375	0.9369	0.9331	0.9228	0.9256	0.9484
$P_{1\%}(t,T)$	0.936	0.9284	0.9092	0.8749	0.8662	0.8896
$P_{5\%}(t,T)$	0.9364	0.9309	0.9159	0.888	0.8833	0.9066
99% Rel. VaR	0.17%	0.91%	2.56%	5.19%	6.41%	6.20%
$T = 30y$, HJM	$t = 1d$	$t = 30d$	$t = 1y$	$t = 5y$	$t = 10y$	$t = 15y$
$\bar{P}(t,T)$	0.9375	0.9369	0.9331	0.9224	0.9256	0.9489
$P_{1\%}(t,T)$	0.936	0.9287	0.9108	0.8805	0.8769	0.903
$P_{5\%}(t,T)$	0.9365	0.931	0.9173	0.8919	0.8906	0.9161
99% Rel. VaR	0.16%	0.87%	2.39%	4.54%	5.27%	4.83%

Table 6.3: Percentiles of a 30 years bond price with the HJM-UFR and HJM frameworks

$T = 40y$, HJM UFR	$t = 1d$	$t = 30d$	$t = 1y$	$t = 5y$	$t = 10y$	$t = 15y$
$\bar{P}(t,T)$	0.7305	0.7301	0.7272	0.719	0.7212	0.739
$P_{1\%}(t,T)$	0.7291	0.7224	0.7056	0.6762	0.6702	0.6849
$P_{5\%}(t,T)$	0.7296	0.7249	0.7123	0.6885	0.6842	0.7
99% Rel. VaR	0.19%	1.05%	2.98%	5.95%	7.07%	7.33%
$T = 40y$, HJM	$t = 1d$	$t = 30d$	$t = 1y$	$t = 5y$	$t = 10y$	$t = 15y$
$\bar{P}(t,T)$	0.7305	0.7302	0.7273	0.7187	0.7211	0.7391
$P_{1\%}(t,T)$	0.729	0.7217	0.703	0.672	0.6631	0.6783
$P_{5\%}(t,T)$	0.7294	0.7241	0.7099	0.6851	0.6799	0.6959
99% Rel. VaR	0.21%	1.16%	3.34%	6.50%	8.04%	8.23%

Table 6.4: Percentiles of a 40 years bond price within the HJM-UFR and HJM frameworks

7 A multi-factor extension

We assume here that forward rates are influenced by p risk-factors. We denote by $\boldsymbol{W}_t = (W_t^1, ..., W_t^p)$, a p-vector of Brownian motions. We consider a p-vector $\boldsymbol{h}(t,T) = (h_1(t,T), ..., h_p(t,T))$ of functions $h_k(t,T) : \mathbb{R}^{2,+} \to [0,1]$ that are continuous and increasing with respect to t and T. We also impose that $h_k(0,T) = 0$ and $\lim_{t\to\infty} h_k(t,T) = 1$ for $k = 1, ..., p$ and for all $T \in \mathbb{R}^+$. The functions $h_k(.)$ are differentiable on $[0, t_\infty)$, where t_∞ is the time at which forward rates reach f_∞. We denote by $\boldsymbol{\omega} = (\omega_1, \ldots, \omega_p)$, a $p-$vector of weights such that $\sum_{k=1}^p \omega_k = 1$. The instantaneous forward rate is ruled by the following equation

$$f(t,T) \;=\; f(0,T) + \left(h(t,T)^\top \boldsymbol{\omega}\right)\left(f_\infty - f(0,T)\right) + \int_0^t \boldsymbol{\sigma}(u,T)^\top d\boldsymbol{W}_u\,, \tag{7.1}$$

where $\boldsymbol{\sigma}(u,T) = (\sigma_1(u,T), ..., \sigma_p(u,T))$ is a vector of p $\mathcal{F}_u$-adapted processes. We can cast this dynamic in the HJM framework and denote by $\int_0^t \alpha(u,T)du$ the drift of forward rates:

$$\begin{aligned}\int_0^t \alpha(u,T)du &= \left(\boldsymbol{h}(t,T)^\top \boldsymbol{\omega}\right)\left(f_\infty - f(0,T)\right)\,, \\ &= \sum_{k=1}^{p} \omega_k\, h_k(t,T)\,\left(f_\infty - f(0,T)\right)\,.\end{aligned} \tag{7.2}$$

Deriving this last equation allows us to infer that the integral of $\alpha(.,.)$ with respect to the maturity is given by

$$\int_t^T \alpha(t,s)ds \;=\; \int_t^T \left(\frac{\partial \boldsymbol{h}(t,s)^\top}{\partial t}\boldsymbol{\omega}\right)\left(f_\infty - f(0,s)\right) ds\,.$$

If we remember that $\boldsymbol{S}(t,T) = -\int_t^T \boldsymbol{\sigma}(t,s)\, ds$, from Proposition 1, the market is arbitrage free if and only if the drift of $f(t,T)$ is related to the volatility through the relation:

$$\begin{aligned}\int_t^T \alpha(t,s)ds &= \frac{1}{2}\boldsymbol{S}(t,T)^\top \boldsymbol{S}(t,T) \\ &= \sum_{k=1}^{p} \frac{1}{2}\left(\int_t^T \sigma_k(t,s)\, ds\right)^2\,.\end{aligned} \tag{7.3}$$

There exist multiple (but non-trivial) solutions to this equation. Nevertheless, a natural one consists to match each terms of sums in Equations (7.2) and (7.3):

$$\omega_k \int_t^T \frac{\partial h_k(t,s)^\top}{\partial t}\left(f_\infty - f(0,s)\right) ds = \frac{1}{2}\left(\int_t^T \sigma_k(t,s)\, ds\right)^2 \quad k = 1, ..., p\,.$$

We infer for $\int_t^T \sigma_k(t,s)\, ds$ a similar expression to the one proposed in Proposition 1 excepted that we have a weighting factor:

$$\int_t^T \sigma_k(t,s)\, ds = \pm\sqrt{2\omega_k \int_t^T \frac{\partial h_k(t,s)^\top}{\partial t}\left(f_\infty - f(0,s)\right) ds} \quad k = 1, ..., p\,. \tag{7.4}$$

Deriving this last equation with respect to T gives the following representation of the volatility:

$$\sigma_k(t,T) \;=\; \pm\frac{\omega_k \frac{\partial h_k(t,T)}{\partial t}\left(f_\infty - f(0,T)\right)}{\sqrt{2\omega_k \int_t^T \frac{\partial h_k(t,s)^\top}{\partial t}\left(f_\infty - f(0,s)\right) ds}} \quad k = 1, ..., p\,. \tag{7.5}$$

Properties of $\sigma_k(t,T)$ for $k = 1, ..., p$ are similar to those of the one factor model. The estimation of the multi-factor model is also done in the same manner. If we denote by $\boldsymbol{\beta}_k$ the vector of parameters

of $h_k(t,T)$ for $k=1,...,p$, their estimates are obtained by minimizing the spread between observed and modeled volatilities of zero-coupon bonds:

$$\widehat{\boldsymbol{\beta}}_k \;=\; \arg\min_{\boldsymbol{\beta}_k} \sum_{j=1}^{d} \left(-\int_t^{t+\tau_j} \sigma_k(t,s)\, ds - \Psi_{j,k}\sqrt{\lambda_k} \right)^2 \quad k=1,...,p. \tag{7.6}$$

As in previous sections, Ψ_k is the k^{th} eigenvector of the covariance matrix of first-order differences of log-bond prices and λ_k is the k^{th} largest eigenvalue. Let us recall that the dimension of Ψ_k is noted d and therefore that $k \leq d$.

To illustrate this section, we fit a bivariate HJM UFR model to ICE swap rates in Euro from the 1/8/2014 to the 21/2/2020. We work with the convergence function defined in Equation (5.4). The weights $\boldsymbol{\omega} = (\omega_1, \omega_2)$ are set a priori and influences the convergence of forward rates to f_∞ since by construction

$$\mathbb{E}^{\mathbb{Q}}\left(f(t,t+\tau)\right) \;=\; f_\infty + \sum_{k=1}^{p} \omega_k\, h_k(t,T)\, \left(f_\infty - f(0,T)\right)\,.$$

There is no criterion to optimize $\boldsymbol{\omega}$ but it seems relevant to link ω_k to the fraction of the total variance explained by the k^{th} principal component, i.e. :

$$\omega_k = \frac{\lambda_k}{\sum_{k=1}^{p}\lambda_k}\;,\; k=1,...,p\,. \tag{7.7}$$

Nevertheless, as underlined in Section 4, the first and second principal components respectively explain 99.12% and 0.77% of the total variance of $\boldsymbol{Y}$ for our data set. Using the rule (7.7) leads to a quasi null second weight. We instead choose $\omega_1 = 0.7$ and $\omega_2 = 0.3$ to emphasize the impact of these weights on the calibration.

Estimates	$h_1(t,T)$, Eq. (5.4)	$h_2(t,T)$, Eq. (5.4)
$\widehat{\beta}_0$	9.3312e-05	9.1800e-06
$\widehat{\beta}_1$	3.0670e-03	1.4398e-06
$\widehat{\beta}_2$	0.0000	8.6285e+01

Table 7.1: Parameter estimates of a bivariate HJM UFR model for convergence functions (5.4).

Table 7.1 reports parameter estimates. Compared to the 1D model and Table 6.1, the presence of the weight ω_1 in Equation (7.5) slightly modifies the parameter estimates. Nevertheless, the goodness of fit remains excellent as underlined by the left plot of Figure 7.1. The right plot shows the evolution of the convergence function, $h_1(t,T)$. It is again very similar to the function obtained for the 1D model, excepted that the amplitude of its increase over 20 years is lower.

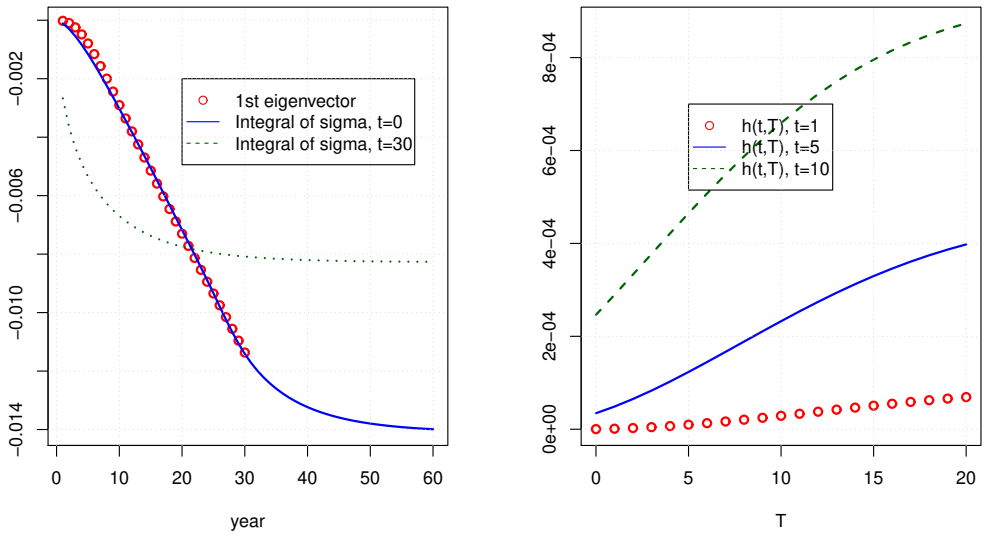

Figure 7.1: Left plot: comparison of $\Psi_{j,1}\sqrt{\lambda_1}$ and $-\int_0^{t+\tau_j}\sigma_1(0,s)ds$. Right plot: convergence functions $h_1(t,T)$.

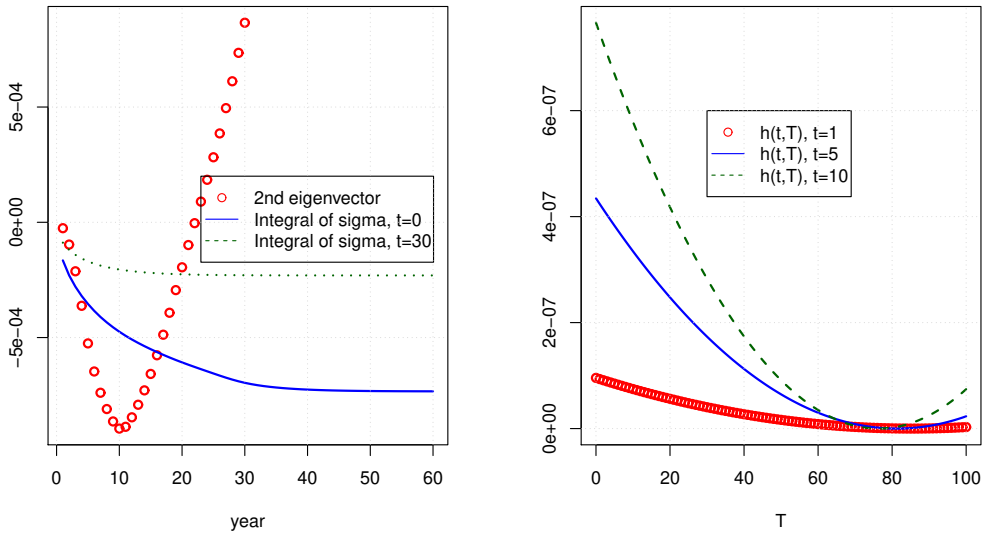

Figure 7.2: Left plot: comparison of $\Psi_{j,2}\sqrt{\lambda_2}$ and $-\int_0^{t+\tau_j}\sigma_2(0,s)ds$. Right plot: convergence functions $h_2(t,T)$.

If we refer to Equation (7.4), the integral $\int_t^T \sigma_k(t,s)\,ds$ is either strictly positive or strictly negative. Therefore, the HJM UFR model cannot explain the flip of sign observed for $\mathbf{\Psi}_2$. We then fit $\sigma_2(t,s)$ to the first 20 positive values of $\mathbf{\Psi}_2$. The result of this calibration is plotted in the left plot of

Figure 7.2. It reveals that the chosen convergence function fails to replicate the hump displayed by $\mathbf{\Psi}_2$. The right plot reveals an interesting feature of $h(t,T)$: the best fit is here obtained with a parabolic convergence function. Does this incapacity to explain a flip of sign in $\mathbf{\Psi}_k$ limit the field of application of the HJM UFR model? To answer this question, we should consider other data sets for which the percentages of the total variance explained by the second and third principal components are higher than those of our data set. In the numerical illustration, we have seen that the first principal component explains 99.12% of the variance and therefore a one factor model is widely sufficient. The second component only generates 0.77% of the total variance and may then be assimilated to a measurement noise.

8 Conclusion

This working note adapts the HJM framework in order to force the convergence of future forward rates toward an ultimate rate (the UFR). This work is motivated by the Solvency II regulation that recommands to use a discount curve adjusted with the Smith-Wilson model. Beyond the last liquid point, the forward rates are forced to converge toward the UFR that is specified by the regulator. In this work, we assume that the drift of forward rates tends to the UFR according to a convergence function. The volatility function of forward rates, $\sigma(t,T)$, is next adapted in order to guarantee the absence of arbitrage. We show that the constraint of convergence implies that this volatility asymptotically vanishes.

The HJM UFR model is next estimated with a standard principal component approach. Applying this procedure to ICE swap rates allows us to draw several interesting conclusions. Firstly, the calibration does not reveal a fast convergence of forward rates toward the UFR. This raises the question of the realism of the assumption made by EIOPA. Secondly, the HJM and the HJM UFR models generate on average quasi similar yield curves. Thirdly, the main difference concerns the term structure of bond volatilities. Within the 1D HJM framework, this volatility is linearly proportional to the maturity of the bond. Whereas in the 1D HJM-UFR model, the term structure of volatilities is curved and tends to be flat for long term maturities.

A comparison of values at risk does not reveal a significant difference between the HJM and HJM UFR models for bonds with maturities up to 30 years and for VaR calculation dates up to 1 year. At longer term, we even observe that the HJM UFR is more conservative than the HJM one. The flattening of bond volatilities has an impact on the bond VaR, only for very long maturities. For a 40 years bond, the value at risk is lower in the HJM UFR than in the HJM model, whatever the chosen time horizon for the VaR.

In theory, the HJM UFR model admits a multi-factors extension. Nevertheless, the model is unable to explain the flip of signs in a principal component of the covariance matrix of first order differences of log-bond prices.

Appendix

Maturity	Swap rate
1	-0.441
2	-0.378
3	-0.363
4	-0.341
5	-0.314
7	-0.247
10	-0.115
15	0.090
20	0.203
25	0.231
30	0.218

Table 8.1: ICE swap rates in Euro on the 21/2/2020.

9 Reference

References

- Amin, K., Morton A., 1994. Implied volatility functions in arbitrage free term structure models. Journal of Financial Economics, 35, 141-180.

- Brigo D. and Mercurio F. 2016. Interest Rate Models. Theory and Practice: With Smile, Inflation and Credit. Springer Berlin Heidelberg.

- Buhler W., Uhrig-Homburg M., Walter U., Weber T., 1999. An empirical comparison of forward rate and spot rate models for valuing interest rate options. The Journal of Finance, 54, 269-305.

- EIOPA 2015. Technical documentation of the methodology to derive eiopa risk-free interest rate term structures. https://eiopa.europa.eu/Publication

- Heath D., Jarrow R., Morton A. 1990. Bond pricing and the term structure of interest rates: a discrete time approximation. *Journal of Financial and Quantitative Analysis*, 25, pp 419-440.

- James J., Weber N. 2000. Interest rate modelling. John Wiley & Sons, Chichester.

- Jorgensen P.L., 2018. An analysis of the Solvency II regulatory framework's Smith-Wilson model for the term Structure of risk-free interest rates. *Journal of Banking and Finance*, 97, 219-237

- Rebonato 2004. Interest–rate term–structure pricing models: a review. Proceedings of The Royal Society A Mathematical Physical and Engineering Sciences, 460 (2043), 667-728.

- Smith A., Wilson T. 2001. Fitting yield curves with long term constraints. London: Bacon and Woodrow.

10 About the serie and the authors...

10.1 The DetraNotes

The Detra Notes are a series of educational papers dedicated to the insurance sector. Those notes are published by members of the Detralytics team and written in a clear and accessible language. The team combines academic expertise and business knowledge. Detralytics was founded to support companies in the advancement of actuarial science and the solving of the profession's future challenges. It is within the scope of this mission that we make our work available through our DetraNotes and FAQctuary's series.

10.2 Authors' biographies

Simon Boigelot

Simon is part of the Talent Accelerator Program (TAP). Prior to joining Detralytics, Simon worked at Belfius Bank as a Senior Quantitative Risk Analyst. His tasks ranged from pricing of financial products to Risk Management. Before that, Simon did two internships, at WTW and Deloitte. Simon holds two Master's degree in Actuarial Sciences and in Civil Engineering, both from UCLouvain

Donatien Hainaut

Donatien Hainaut is Scientific Director at Detralytics Donatien and professor at UCLouvain where he is Director of the new Master program in Data Science, statistical orientation. Prior to this he held several positions as associate professor at Rennes School of Business and the ENSAE in Paris. He also has several field experiences having worked as Risk Officer, Quantitative Analyst and ALM Officer.

Donatien is a Qualified Actuary and holds a PhD in the area of Assets and Liability Management. His current research focuses on contagion mechanism in stochastic processes and applications of neural networks to insurance.

Detra²lytics

Expertise and innovation at the service of your future

www.detralytics.com - info@detralytics.eu